

Unital Qubit Queue-channels: Classical Capacity and Product Decoding

Vikesh Siddhu, Avhishek Chatterjee, Krishna Jagannathan, Prabha Mandayam, Sridhar Tayur

Abstract

Quantum queue-channels arise naturally in the context of buffering in quantum networks, wherein the noise suffered by the quantum states depends on the time spent waiting in the buffer. It has been shown that the upper-bound on the classical capacity of an additive queue-channel has a simple expression, and is achievable for the erasure and depolarizing channels [1]. In this paper, we characterise the classical capacity for the class of unital qubit queue-channels, and show that a simple product (non-entangled) decoding strategy is capacity-achieving. As an intermediate result, we derive an explicit capacity achieving product decoding strategy for any i.i.d. unital qubit channel, which could be of independent interest. As an important special case, we also derive the capacity and optimal decoding strategies for a symmetric generalized amplitude damping (GAD) queue-channel. Our results provide useful insights towards designing practical quantum communication networks, and highlight the need to explicitly model the impact of buffering.

I. INTRODUCTION

There is considerable and growing interest in designing and setting up large-scale quantum communication networks [2], [3]. To that end, understanding the fundamental capacity limits of quantum communications in the presence of noise is of practical importance. In this context, the inevitable buffering of quantum states during communication tasks acts as an additional source of decoherence. One concrete example of such buffering occurs at intermediate nodes or quantum repeaters, where quantum states have to be stored for a certain *waiting time* until they are processed and transmitted again [4]. Indeed, while quantum states wait in buffer for transmission, they continue to interact with the environment, and suffer a *waiting time dependent* decoherence [5], [6]. In fact, the longer a qubit waits in a buffer, the more it decoheres.

To characterise the impact of buffering on quantum communication, researchers have recently combined queuing models with quantum noise models [1]. In particular, the buffering process inherently introduces correlations across the noise process experienced by consecutive qubits, since the waiting times are correlated according to the queuing

V. Siddhu was with JILA, University of Colorado/NIST, 440 UCB, Boulder, CO 80309, USA (email: vsiddhu@protonmail.com). He is presently with IBM Quantum, IBM T.J. Watson Research Center, New York.

A. Chatterjee and K. Jagannathan are with the Department of Electrical Engineering, IIT Madras, Chennai, India (e-mail: {avhishek, krishnaj}@ee.iitm.ac.in).

P. Mandayam is with the Department of Physics, IIT Madras, Chennai, India (e-mail: prabhamd@iitm.ac.in).

S. Tayur is with the Quantum Computing Group, Tepper School of Business, and Department of ECE, Carnegie Mellon University, Pittsburgh PA 15213, USA (email: stayur@cmu.edu).

dynamics. Thus, to properly characterise the decoherence introduced due to buffering, we need to look ‘beyond i.i.d.’ quantum channels and noise models.

Unital qubit channels are ubiquitous models for decoherence [7], [8] in the communication medium as well as in the buffer. Though the former mode of decoherence has been the main topic of interest in quantum Shannon theory, recent research has started to focus on the impact of the buffering on the design of a practical quantum communication system [1], [4]–[6].

The i.i.d. unital channel has been studied extensively and its classical capacity has been characterized [9]–[14]. The classical capacity is known to be additive and is achieved by non-entangled (product) encoding. However, to the best of our knowledge, the following questions have not been resolved: (a) can product *decoding* achieve the classical capacity of the channel, and (b) if so, is there an explicit quantum measurement that achieves the capacity? These questions are well-motivated regardless of any buffering considerations, because entangled measurement (non-product decoding) requires a reliable quantum processor. Motivated by the practical issue of decoherence during buffering, we further ask: what is the impact of decoherence at the transmission buffer on the classical capacity and does it change the answers to questions (a) and (b)?

A. Related Work

Our work interleaves different aspects of quantum communication networks, from quantum Shannon theory to queuing theory. In quantum Shannon theory, one studies ultimate limits for transmitting information in the presence of quantum noise. One simple model of study is transmission of classical information across qubits experiencing i.i.d noise. However even this simple model can exhibit a variety of complex behaviour [15]–[17]. The qubit generalized amplitude damping channel (GADC) is a relevant model of noise in a variety of physical contexts including communication over optical fibers or free space [18]–[21], T_1 relaxation due to coupling of spins with a high temperature environment [22]–[24], and super-conducting based quantum computing [25]. Quantum capacities of the i.i.d. GADC have been studied (see [26] and reference therein). Of particular interest to us are expressions for the Holevo information of the GADC, found in [27] using techniques from [28], [29], and channel parameters [26] where additivity of the GADC Holevo information is known. While the primary focus of quantum Shannon theory [30] has been to study the classical and quantum capacities of stationary, memoryless quantum channels [8], recently there has been a spurt of activity in characterizing the capacities of quantum channels in non-stationary, correlated settings. We refer to [31] for a recent review of the different capacity results obtained in a context of quantum channels that are not independent or identical across channel uses. In particular, we focus on the quantum information-spectrum approach in [32], which provides bounds on the classical capacity of a general, non-i.i.d. sequence of quantum channels. The idea of a quantum queue-channel was originally proposed in [33] as a way to model and study the effect of decoherence due to buffering or queuing in quantum information processing tasks. The classical capacity of quantum queue-channels has been studied for certain classes of quantum channels, and a general upper bound is known for additive quantum queue-channels, additionally the upper bound can be achieved for for the *erasure* and *depolarising* queue-channels [1]. The effect of queuing-dependent errors on classical channels has been studied earlier [34], with motivation drawn from crowd-sourcing. More recently, a

dynamic programming based framework for characterising the queuing delay of quantum data with finite memory size has been proposed in [35]. Finally, we note that ideas of queuing theory have also been used to study aspects of entanglement distribution over quantum networks such as routing [36], switching, and buffering [37].

B. Our Contributions:

We show that the upper-bound on the classical capacity of additive queue-channel is achievable for any unital qubit queue-channel if the encoder has non-causal side information regarding the waiting times of the qubits. In the absence of this side information, we show that for the class of unital qubit queue-channels that are ‘Pauli-ordered,’ the same upper-bound can be achieved. In both cases, we show that non-entangled projective measurements can achieve the capacity and provide explicit descriptions of the encoders and the projective measurements. As an intermediate result, we derive a capacity achieving non-entangled projective measurement for any i.i.d. unital qubit channel. To the best of our knowledge, this result has not been discussed in the literature, and could be of independent interest.

An important example of a unital channel is the symmetric generalized amplitude damping (GAD) channel. The GADC, $\mathcal{A}_{p,n}$, is typically parametrized by two quantities, n and p , both between zero and one. At $n = 1/2$, one obtains a symmetric GADC which is unital, however for other values of n the channel is not unital. We construct three different ‘natural’ induced channels and find one of them, \mathcal{N}_3 a binary symmetric channel, to have the largest Shannon capacity $C(\mathcal{N}_3)$ for all n and p . Typically, $C(\mathcal{N}_3)$ is found to be less than the GAD channel’s Holevo information, however at $n = 1/2$ we find $C(\mathcal{N}_3)$ equals the Holevo information for all p . Next, we study a symmetric GAD queue-channel with $n = 1/2$, and the parameter p is made an explicit function of the waiting time w of each qubit. Such a symmetric GAD queue channel is unital and hence additive, which enables the use of the capacity upper bound obtained in [1]. Further, we propose a specific encoding for the GAD queue channel, which induces a binary symmetric classical queue channel. We show that an achievable rate of this binary symmetric queue channel matches the upper bound enforced by additivity arguments, thus settling the capacity of the GAD queue channel, and giving us a fully classical capacity achieving scheme for the encoder and decoder. Finally, we obtain useful insights for designing practical quantum communication systems by employing queuing theoretic analysis on the queue-channel capacity results.

The paper is organized as follows. In the Sec. **I-A** we discuss related work. To keep this discussion somewhat self-contained, in Sec. **II**, we provide an extended discussion of induced channels, classical capacities of quantum channels, and non-i.i.d queue-channel capacities. Sec. **III** discusses unital qubit queue-channels and includes a capacity achieving product encoding-decoding strategy for i.i.d. unital channels (see Th. 1). In Sec. **IV-A**, we analyze the generalized amplitude damping channel (GADC). Here we discuss and compare capacities of various natural choices for induced channels of a GADC (see Fig. 2). In Sec. **IV-D** we discuss the queue-channel capacity of the symmetric GADC. We offer useful design insights by analyzing and numerically plotting (see Fig. 3) the capacity expression. Sec. **V** contains a brief discussion and outlines potentially interesting future directions.

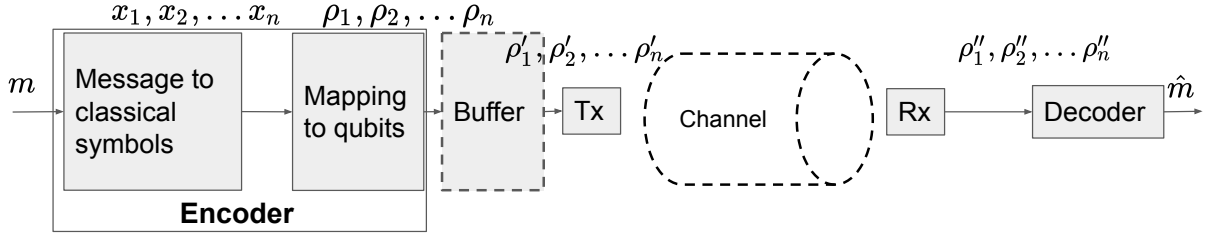


Fig. 1: Qubit ρ_i decoheres to ρ'_i while waiting in the buffer for transmission. This further decoheres to ρ''_i while passing through the channel. Decoherence in the buffer depends on the waiting time and results in non-i.i.d. "effective" decoherence.

II. PRELIMINARIES

A. Classical and Quantum Channels

A random variable, X , taking discrete value x from a finite set \mathcal{X} with $p(x) := \Pr(X = x)$ has Shannon entropy $H(X) = -\sum_{x \in \mathcal{X}} p(x) \log_2 p(x)$. A discrete memoryless channel N taking $x \in \mathcal{X}$ to $y \in \mathcal{Y}$ with conditional probability $p(y|x) := \Pr(Y = y|X = x)$ has channel capacity

$$C_{\text{Shan}}(N) = \max_{p(x)} I(X; Y), \quad (1)$$

where $I(X; Y) := H(X) + H(Y) - H(X, Y)$ is the mutual information between input X and output Y . A binary symmetric channel (BSC) with flip probability q , is defined by the conditional probability distribution $p(0|0) = 1 - q, p(1|0) = q, p(0|1) = q, p(1|1) = 1 - q$, where $0 \leq q \leq 1$; it has capacity $1 - h(q)$, where $h(q) = -[q \log_2 q + (1 - q) \log_2 (1 - q)]$ is the binary entropy function. A binary asymmetric channel (BAC), defined by the conditional probability distribution $p(0|0) = 1 - q, p(1|0) = q, p(0|1) = r$, and $p(1|1) = 1 - r$, has capacity

$$C_{\text{Shan}}(\text{BAC}(q, r)) = \frac{1}{1 - s - t} (sh(t) - (1 - t)h(s)) + \log_2 \left(1 + 2^{\frac{h(s) - h(t)}{1 - s - t}} \right), \quad (2)$$

where $s = \min(q, r)$ and $t = \max(q, r)$.

Let \mathcal{H} denote a finite dimensional Hilbert space, $\mathcal{L}(\mathcal{H})$ denote the space of bounded linear operators on \mathcal{H} . A density operator ρ is a positive semi-definite operator in $\mathcal{L}(\mathcal{H})$ with unit trace, $\text{Tr}(\rho) = 1$. A classical quantum (c-q) channel, $\mathcal{E} : \mathcal{X} \mapsto \mathcal{L}(\mathcal{H})$ maps a symbol $x \in \mathcal{X}$ to a density operator $\rho(x) \in \mathcal{L}(\mathcal{H})$. Measuring $\rho(x)$ and recording the measurement outcome $y \in \mathcal{Y}$ can be represented by a map $\mathcal{D} : \mathcal{L}(\mathcal{H}) \mapsto \mathcal{Y}$. This measurement can be described using a POVM, a collection of positive operators in $\mathcal{L}(\mathcal{H})$ that sum to the identity. Suppose the POVM $\{\Lambda(y)\}$ specifies \mathcal{D} ; then any input $x \in \mathcal{X}$ is decoded as y with conditional probability,

$$p(y|x) = \Pr(Y = y|X = x) = \text{Tr}(\Lambda(y)\rho(x)). \quad (3)$$

This conditional probability defines an *induced channel* $N : \mathcal{X} \mapsto \mathcal{Y}$ with capacity $C_{\text{Shan}}(N)$ (see Ch.20 in [30]). For a fixed \mathcal{E} , maximizing this capacity over choice of decodings \mathcal{D} defines the Shannon capacity of \mathcal{E} ,

$$C_{\text{Shan}}(\mathcal{E}) = \max_{\mathcal{D}} C_{\text{Shan}}(N) = \max_{\mathcal{D}, p(x)} I(Y; X). \quad (4)$$

For a fixed $p(x)$ and output alphabet \mathcal{Y} , $I(X; Y)$ is convex in $p(y|x)$, and $p(y|x)$ is linear in the decoding POVM $\{\Lambda(y)\}$ specifying \mathcal{D} . The resulting convexity of $I(X; Y)$ in \mathcal{D} , for fixed \mathcal{Y} , is one reason due to which the capacity $C_{\text{Shan}}(\mathcal{E})$ is non-trivial to compute. A larger capacity can be obtained using a fixed product encoding $\mathcal{E} : \mathcal{X} \mapsto \mathcal{L}(\mathcal{H})$ by allowing for decoding $\mathcal{D}_k : \mathcal{L}(\mathcal{H}^{\otimes k}) \mapsto \mathcal{Y}^{\otimes k}$ that may jointly measure k encoded states. Such decoding \mathcal{D}_k defines an induced channel N_k . Maximizing the channel mutual information $\mathcal{I}(N_k)$ over all decodings \mathcal{D}_k defines $\mathcal{I}^{(k)}(\mathcal{E})$. Due to the presence of entanglement in the joint decoding measurements, one may have $\mathcal{I}^{(k)}(\mathcal{E}) \geq k\mathcal{I}^{(1)}(\mathcal{E})$. Due to this type of *super-additivity*, a proper definition of the capacity C_{pj} of sending classical information using product encoding \mathcal{E} and joint decoding is given by a *multi-letter* formula,

$$C_{pj} = \lim_{k \rightarrow \infty} \frac{1}{k} \mathcal{I}^{(k)}(\mathcal{E}). \quad (5)$$

Remarkably, the Holevo-Schumacher-Westmoreland theorem [38], [39] gives the above multi-letter expression a *single-letter* form; that is,

$$C_{pj}(\mathcal{E}) = \chi^{(1)}(\mathcal{E}) := \max_{\{p(x)\}} \chi(p(x), \rho(x)), \quad (6)$$

where the Holevo quantity,

$$\chi(p(x), \rho(x)) = S\left(\sum_{x \in \mathcal{X}} p(x)\rho(x)\right) - \sum_x p(x)S(\rho(x)), \quad (7)$$

and $S(\rho) = -\text{Tr}(\rho \log \rho)$, is the von-Neumann entropy of a density operator ρ . Due to the close connection between C_{pj} and χ , sometimes $C_{pj}(\mathcal{E})$ is also denoted by $C_\chi(\mathcal{E})$. There are cases where $C_\chi(\mathcal{E})$ is strictly greater than $C_{\text{Shan}}(\mathcal{E})$ [40], [41]. However, much remains unknown about when and how such separations occur.

B. Classical Capacities of a Quantum Channel

A quantum channel $\mathcal{B} : \mathcal{L}(\mathcal{H}_a) \mapsto \mathcal{L}(\mathcal{H}_b)$ is a completely positive trace preserving (CPTP) map. The Shannon capacity of \mathcal{B} ,

$$C_{\text{Shan}}(\mathcal{B}) = \max_{\mathcal{E}, \mathcal{D}} \mathcal{I}(N) = \max_{\{\mathcal{E}, \mathcal{D}\}} \max_{p(x)} I(X; Y), \quad (8)$$

where $N : X \mapsto Y$ is an induced channel obtained by using product encoding $\mathcal{E} : \mathcal{X} \mapsto \mathcal{L}(\mathcal{H}_a)$ and product decoding $\mathcal{D} : \mathcal{L}(\mathcal{H}_b) \mapsto \mathcal{Y}$. Allowing for joint encodings while restricting the decoder to product decodings does not increase the channel's ability to send classical information beyond the channel's Shannon capacity, i.e., $C_{jp}(\mathcal{B}) = C_{\text{Shan}}(\mathcal{B})$ [42]. The Shannon capacity is bounded from above by $C_{pj}(\mathcal{B})$, sometimes called the Holevo capacity or the product state capacity of \mathcal{B} . A multi-letter expression of the form (5) for $C_{pj}(\mathcal{B})$ can be shown to equal to a single-letter formula,

$$C_{pj}(\mathcal{B}) = \chi^{(1)}(\mathcal{B}) := \max_{\{\rho_a(x), p(x)\}} \chi(p(x), \rho_b(x)), \quad (9)$$

where $\rho_b(x) = \mathcal{B}(\rho_a(x))$. The most general capacity of a channel $C_{jj}(\mathcal{B})$, sometimes called the *classical capacity* of \mathcal{B} allows for joint encoding $\mathcal{E}_k : \mathcal{X}^{\times k} \mapsto \mathcal{L}(\mathcal{H}_a^{\otimes k})$ and decoding $\mathcal{D}_k : \mathcal{L}(\mathcal{H}_b^{\otimes k}) \mapsto \mathcal{Y}^{\times k}$. This encoding-decoding results in an induced channel $\tilde{\mathcal{N}}_k : X^{\times k} \mapsto Y^{\times k}$. Maximizing the mutual information of this induced channel over all \mathcal{E}_k and \mathcal{D}_k gives $\tilde{\mathcal{I}}^k(\mathcal{B})$. This quantity can be super-additive, as a result $C_{jj}(\mathcal{B})$ is defined by a multi-letter expression of the form (5). Using the product state capacity $\chi^{(1)}(\mathcal{B})$ (9), $C_{jj}(\mathcal{B})$ can be written as follows,

$$C_{jj}(\mathcal{B}) = \lim_{k \rightarrow \infty} \frac{1}{k} \chi^{(1)}(\mathcal{B}^{\otimes k}) := \chi(\mathcal{B}). \quad (10)$$

In general, the limit in (10) is required because the product state capacity can be non-additive [43]; that is, for any two quantum channels \mathcal{B} and \mathcal{B}' , the inequality,

$$\chi^{(1)}(\mathcal{B} \otimes \mathcal{B}') \geq \chi^{(1)}(\mathcal{B}) + \chi^{(1)}(\mathcal{B}'), \quad (11)$$

can be strict. For certain special classes of channels, the Holevo information is known to be additive; that is, the inequality above becomes an equality when \mathcal{B}' is any channel and \mathcal{B} belongs to a special class of channels that includes unital qubit channels [9], depolarizing channels [44], Hadamard channels [45], and entanglement breaking channels [46].

C. Classical capacity of non-i.i.d. quantum channels

Much of the focus in quantum Shannon theory is on quantum channels that are *independent and identically distributed (i.i.d.)* across multiple uses. As mentioned in Sec. I, the effective channel seen by qubits in the presence of decoherence in the transmission buffer is non-i.i.d. Characterizing the capacity is a harder problem in such a setting. In the classical setting, a capacity formula for this general non-i.i.d. setting was obtained using the information-spectrum method [47], [48]. This technique was adapted to the quantum setting in [32], and a general capacity formula was obtained for the classical capacity of a quantum channel.

1) *The Quantum inf-information rate:* Recall that a quantum channel is defined as a completely positive, trace-preserving map $\mathcal{B} : \mathcal{H}_a \mapsto \mathcal{H}_b$ from the "input" Hilbert space \mathcal{H}_a to the "output" Hilbert space \mathcal{H}_b . Consider a sequence of quantum channels $\vec{\mathcal{N}} \equiv \{\mathcal{N}^{(n)}\}_{n=1}^{\infty}$. Let \vec{P} denote the totality of sequences $\{P^n(X^n)\}_{n=1}^{\infty}$ of probability distributions (with finite support) over input sequences X^n , and $\vec{\rho}$ denote the sequences of states ρ_{X^n} corresponding to the encoding $X^n \rightarrow \rho_{X^n}$. For any $a \in \mathbb{R}^+$ and n , we define the operator,

$$\mathcal{O}_{\{P^n(X^n), \rho_{X^n}\}}(a) = \mathcal{N}^{(n)}(\rho_{X^n}) - e^{an} \sum_{X^n \in \mathcal{X}^{(n)}} P^n(X^n) \mathcal{N}^{(n)}(\rho_{X^n}).$$

Further, let $\{\mathcal{O}_{\{P^n(X^n), \rho_{X^n}\}}(a) > 0\}$ denote the projector onto the positive eigenspace of the operator $\mathcal{O}_{\{P^n(X^n), \rho_{X^n}\}}(a)$.

Definition 1. *The quantum inf-information rate [32] $\underline{\mathbf{I}}(\{\vec{P}, \vec{\rho}\}, \vec{\mathcal{N}})$ is defined as,*

$$\underline{\mathbf{I}}(\{\vec{P}, \vec{\rho}\}, \vec{\mathcal{N}}) = \sup \left\{ a \in \mathbb{R}^+ \left| \lim_{n \rightarrow \infty} \sum_{X^n \in \mathcal{X}^{(n)}} P^n(X^n) \text{tr} \left[\mathcal{N}^{(n)}(\rho_{X^n}) \{\mathcal{O}_{\{P^n(X^n), \rho_{X^n}\}}(a) > 0\} \right] = 1 \right. \right\}. \quad (12)$$

This is the quantum analogue of the classical inf-information rate originally defined in [47], [48]. The central result of [32] is to show that the classical capacity of the channel sequence $\vec{\mathcal{N}}$ is given by

$$C = \sup_{\{\vec{P}, \vec{\rho}\}} \mathbf{I}(\{\vec{P}, \vec{\rho}\}, \vec{\mathcal{N}}).$$

III. UNITAL QUBIT QUEUE-CHANNELS

A unital qubit channel Φ satisfies $\Phi(I) = I$ where I is the 2×2 identity operator. By itself, the channel describes i.i.d. noise. The capacity of sending classical information in this i.i.d. setting was discussed in Sec. II-B, where we mentioned that the product state classical capacity of Φ is additive and thus the channel's capacity, $\chi(\Phi)$, can be achieved using product encoding.

A unital qubit queue-channel models the total decoherence experienced by the qubits while waiting in the buffer for transmission and passing through the channel. Each qubit experiences a (potentially) different unital qubit channel Φ_W parametrized by the random time W that it spends in the buffer. In this case, for the transmitted state $\rho_{12\dots k}$, the output state would be $(\Phi_{W_1} \otimes \Phi_{W_2} \cdots \Phi_{W_k})(\rho_{12\dots k})$, if the waiting times $W^k = (W_1, W_2, \dots, W_k)$ are known at the receiver. Examples of unital qubit queue-channels include the depolarising queue-channels [1] and the symmetric generalized amplitude damping queue-channel (see Sec. III-C).

The buffering process is modeled as a continuous-time single-server queue. To be specific, the single-server queue is characterised by (i) A server that processes the qubits in the order in which they arrive, that is in a First Come First Served (FCFS) fashion*, and (ii) An "unlimited buffer" — that is, there is no limit on the number of qubits that can wait to be transmitted. We denote the time between preparation of the i th and $i + 1$ th qubits by A_i , where A_i are i.i.d. random variables. These A_i s are viewed as inter-arrival times of a point process of rate λ , where $\mathbb{E}[A_i] = 1/\lambda$. The "service time," or the time taken to transmit qubit i , is denoted by S_i , where $\{S_i\}$ are also assumed to be i.i.d. random variables, independent of the inter-arrival times $A_i, i \geq 1$. The "service rate" of the qubits is denoted by $\mu = 1/\mathbb{E}[S_i]$. We assume that $\lambda < \mu$ (i.e., mean transmission time is strictly less than the mean preparation time) to ensure stability of the queue. Qubit 1 has a waiting time $W_1 = S_1$. The waiting times of the other qubits can be obtained using the well known Lindley's recursion:

$$W_{i+1} = \max(W_i - A_i, 0) + S_{i+1}.$$

In queuing parlance, the above system describes a continuous-time $G/G/1$ queue. Under mild conditions, the sequence $\{W_i\}$ for a stable $G/G/1$ queue is *ergodic*, and reaches a *stationary distribution* π . We assume that the waiting times $\{W_i\}$ of the qubits are *available* at the receiver during decoding.

An important difference between the queue-channel introduced above and the usual i.i.d. channels is that this channel is a part of continuous time dynamics. Hence, the usual notion of capacity per *channel use* for i.i.d. channels is not pertinent here. As mentioned before, the above channel model is closely related to quantum queue-channels studied in [1]. So, we first do a short review of the notion of capacity per *unit time* and some relevant capacity results in [1].

*The FCFS assumption is not required for our results to hold, but it helps the exposition.

A. Classical capacity of unital quantum queue-channels

Definition 2. A rate R is called an achievable rate for a quantum queue-channel if there exists a sequence of $(n, 2^{RT_n})$ quantum codes with probability of error $P_e^{(n)} \rightarrow 0$ as $n \rightarrow \infty$ and $\mathbf{E} \left[\sum_{i=1}^{n-1} A_i + W_n \right] \leq T_n$.

Definition 3. The information capacity of the queue-channel is the supremum of all achievable rates for a given arrival and service process, and is measured in bits per unit time.

Note that the information capacity of the queue-channel depends on the arrival process, the service process, and the noise model.

As discussed in Sec. I, in this paper, we derive the capacity of this channel and show that product encoding and product decoding achieve that capacity. Towards this, an important intermediate step of (possibly) independent interest is to design an explicit product encoding and product decoding strategy for i.i.d. unital qubit channels.

B. Product Encoding/Decoding for i.i.d. Unital Qubit Channels

It is well known that product encoding achieves the classical capacity of an i.i.d. unital qubit channel, which is equal to the Holevo information [9]. In this section, we show that product decoding is sufficient to achieve that capacity and provide an explicit capacity achieving product encoding and decoding strategy. To the best of our knowledge, this explicit result is not available in the current literature.

The classical capacity of an i.i.d. unital qubit channel Φ is given by the Holevo information [9]

$$\chi(\Phi) = \sup_{p, \rho, \rho'} (S(\Phi(p\rho + (1-p)\rho')) - pS(\Phi(\rho)) - (1-p)S(\Phi(\rho'))). \quad (13)$$

1) *Product encoding and decoding:* For a unital qubit channel Φ , let

$$M_\Phi = \sup_{\rho} \|\Phi(\rho)\|, \quad (14)$$

where $\|\cdot\|$ is the operator norm (it equals the largest eigenvalue of a density operator).

We define \mathcal{R}_Φ to be the set of states that achieves the supremum in (14), i.e., for any $\rho \in \mathcal{R}_\Phi$, $M_\Phi = \|\Phi(\rho)\|$.

For any state $\rho \in \mathcal{R}_\Phi$, we define $\Gamma_{\Phi, \rho}$ to be the set of states such that for any $\tau \in \Gamma_{\Phi, \rho}$

$$M_\Phi = \text{Tr}(\Phi(\rho)\tau). \quad (15)$$

Message to classical bits: Consider the classical binary symmetric channel (BSC) with cross-over probability M_Φ and choose any capacity achieving encoder and decoder. For example, one can choose the well known random coding and typical decoding, or an appropriate polar code and the corresponding decoder.

Encoding classical bits to quantum states: For sending a message over the unital channel, first map the message to an appropriate classical binary codeword from the chosen classical codebook. Then map symbol 0 to a state $\rho^* \in \mathcal{R}_\Phi$ and symbol 1 to $I - \rho^*$, and transmit over the unital channel.

Decoding quantum states: At the receiver, use projection measurements $\{P_0 = I - \tau^*, P_1 = \tau^*\}$, where $\tau^* \in \Gamma_{\Phi, \rho^*}$, and obtain a sequence of 0 and 1. Then, use the classical decoder chosen for the BSC(M_Φ).

Theorem 1. *The above product encoding and decoding strategy for the unital qubit channel achieves the capacity in (13).*

Proof. First, we prove that the above encoding and decoding across an i.i.d. unital qubit channel results in a classical i.i.d. BSC (M_Φ). The rest follows using the fact that $\chi(\Phi) = 1 - h(M_\Phi)$ [9] and $1 - h(M_\Phi)$ is the Shannon capacity of BSC(M_Φ).

The probability that bit 0 is decoded as bit 1 is equal to the probability that the projective measurement $\{P_0, P_1\}$ on $\Phi(\rho^*)$ gives 1. Similarly, the probability that bit 1 is decoded as bit 0 is same as the probability of the event that the projective measurement on $\Phi(I - \rho^*)$ gives 0. The second probability is given by

$$\begin{aligned} & \text{Tr}((I - \tau^*)\Phi(I - \rho^*)) \\ &= \text{Tr}((I - \tau^*)(I - \Phi(\rho^*))) \quad (\text{unital channel}) \\ &= \text{Tr}(I - \tau^* - \Phi(\rho^*) + \tau^*\Phi(\rho^*)) \\ &= \text{Tr}(\tau^*\Phi(\rho^*)). \end{aligned}$$

This expression, however, is exactly equal to first probability, which in turn is given by

$$\begin{aligned} & \text{Tr}(\tau^*\Phi(\rho^*)) \\ &= \sup_{\tau: \text{pure state}} \text{Tr}(\Phi(\rho^*)\tau) \\ &= \|\Phi(\rho^*)\| \quad (\text{by the defn. of operator norm}) \\ &= M_\Phi. \end{aligned}$$

This completes the proof. ■

The main insight from the above theorem is summarized in the following remark.

Remark 1. *Every unital qubit channel has an induced binary symmetric channel whose Shannon capacity equals the classical capacity of the unital qubit channel.*

Next, building on the above insight and Theorem 4 in [1], we study unital qubit queue-channels.

C. Capacity of Unital Qubit Queue-channels

We start with the capacity upper-bound in [1], which is applicable to any additive queue-channel. We assume that the waiting times of the qubits are *available* at the receiver during decoding.

Theorem 2 ([1], Theorem 1). *The classical capacity of a unital qubit queue-channel is upper-bounded by $\lambda \mathbf{E}_\pi \chi(\Phi_W)$, irrespective of whether the encoder knows the waiting times or does not know the waiting times. Here, \mathbf{E}_π is expectation with respect to the stationary distribution π of $\{W_i\}$.*

Proof. The case where waiting times are not known at the encoder is a direct re-statement from [1]. The other case follows by noting the fact that in deriving the upper-bound in [1], the encoder was allowed access to the additional side information regarding the waiting times. ■

We study encoding and decoding strategies that achieve the above bound in both settings. We start with the simpler setting where encoder knows the waiting times and later we study the more practical setting, where the encoder does not know the waiting times.

1) *Encoder knows waiting times:* Knowledge of the future parameters of a time-varying channel at the receiver is called non-causal side information. This is not practical when the channel variation is fast and unpredictable (i.i.d. like). However, as the waiting times result into a Markov process, such an assumption is not so impractical. In certain slowly varying queues, the waiting times can be predicted within a reasonable accuracy. In this setting, the product encoding and product decoding strategy is similar to the one considered in Sec. III-B. However, some modifications are necessary to address the non-i.i.d. nature of the queue-channel.

First, we introduce a modified version of (13). For an unital qubit channel parametrized by waiting time W , let

$$\begin{aligned} M_{\Phi_W} &= \sup_{\rho} \|\Phi_W(\rho)\|, \\ \mathcal{R}_{\Phi_W} &= \{\rho : \|\Phi_W(\rho)\| = M_{\Phi_W}\}, \\ \Gamma_{\Phi_W, \rho} &= \{\tau : \text{Tr}(\tau\Phi(\rho)) = M_{\Phi_W}\} \text{ for } \rho \in \mathcal{R}_{\Phi_W}. \end{aligned} \quad (16)$$

Message to classical bits: Pick any capacity achieving encoder and decoder for the classical binary symmetric queue-channel $\{\text{BSC}(M_{\Phi_{W_i}})\}$. A detailed discussion on this channel can be found in [1].

Product encoding and decoding of qubits: The encoder and the decoder agree a priori on a choice of $\rho_W \in \mathcal{R}_{\Phi_W}$ for all $W \geq 0$. The encoder maps the i th classical bit to ρ_{W_i} or $I - \rho_{W_i}$, depending on whether it is 0 or 1, respectively. For the i th quantum state at the output of the channel, the decoder uses the projective measurement $\{I - \tau_{W_i}, \tau_{W_i}\}$, where $\tau_{W_i} \in \Gamma_{\Phi_{W_i}, \rho_{W_i}}$.

Theorem 3. *The above product encoding and product decoding strategy for unital qubit queue-channel achieves the capacity upper-bound in Theorem 2.*

Proof. Using the steps from the proof of Theorem 1, it directly follows that the above strategy converts the unital qubit queue-channel into a binary symmetric queue-channel $\{\text{BSC}(M_{\Phi_{W_i}})\}$. Rest follows from Theorem 4 in [1]. ■

2) *Encoder does not know waiting times:* In this setting the queue evolution cannot be predicted and hence, the encoder has no knowledge of $\{W_i\}$. This is a more prevalent setting in quantum communication. In many practical quantum communication systems, the encoding and the decoding has to be chosen at time zero, and cannot be adapted according to the queue evolution. We show that, in this setting, again a simple product encoder and product decoder achieves capacity for a large class of unital qubit queue-channels.

We obtain two results in this setting. First, we show that for a class of unital qubit queue-channels with certain Pauli decomposition characteristics whose Pauli decompositions satisfy a certain invariant ordering, the capacity can be achieved by product encoding and decoding in terms of Pauli matrices (Theorem 5 and Lemma 6). This class of channels includes the well known depolarizing channels, the symmetric generalized amplitude damping channel and other Pauli channels such as bit-flip and phase-flip channels. Second, we further introduce a broader class of unital qubit queue-channels which can be characterized without using the Pauli decomposition for which product encoding and decoding is optimal, independent of their Pauli noise characteristics (Theorem 7).

Let us consider a *family* of i.i.d. unital qubit channels $\{\Phi_w\}$, parametrized by a non-negative real number w . This means that the channel acts on any joint state $\rho_{12\dots k}$ as

$$(\Phi_w \otimes \Phi_w \otimes \dots \otimes \Phi_w)(\rho_{12\dots k}),$$

where the parameter w determines the map. As discussed in Theorem 1, the classical capacity of this channel is achieved by the product encoding: $0 \rightarrow \rho_w^*$ and $1 \rightarrow I - \rho_w^*$, and product decoding using the projectors $\{\tau_w^*, I - \tau_w^*\}$, where

$$\rho_w^* \in \mathcal{R}_{\Phi_w} \text{ and } \tau_w^* \in \Gamma_{\Phi_w, \rho_w^*}.$$

Further, the classical capacity of this unital qubit channel is equal to the Shannon capacity of a binary symmetric channel with crossover probability $M_{\Phi_w} = \|\Phi_w(\rho_w^*)\|$.

It is well known that any qubit state ρ can be expressed as linear combination of the Pauli matrices σ_i , $i = 1, 2, 3$, and I . This leads to three natural induced classical channels for any qubit channel: map 0 and 1, respectively, to $\frac{I+\sigma_i}{2}$ and $\frac{I-\sigma_i}{2}$, the projectors onto the two eigenvectors of σ_i , and measure using these same projectors. For the i.i.d. unital qubit channel Φ_w , parametrized by w , this leads to three induced binary symmetric channels $B_i(w)$, $i = 1, 2, 3$.

A family of i.i.d. unital qubit channels $\{\Phi_w\}$ and an unital qubit queue-channel are closely related. In a unital qubit queue-channel, each qubit i sees a different unital qubit channel depending on its waiting time W_i . Thus, any unital qubit queue-channel can be described using a family of i.i.d. unital qubit channels $\{\Phi_w\}$, such that the channel seen by any qubit i is Φ_w , where $w = W_i$. Clearly, the physical environment of the buffer decides the nature of the queue-channel and thus, determines the family $\{\Phi_w\}$ that corresponds to it.

Definition 4. We call a unital qubit queue-channel **Pauli-ordered** if the ordering of the Shannon capacities of the induced channels $B_1(w)$, $B_2(w)$ and $B_3(w)$ of the corresponding family of the i.i.d. unital qubit channels $\{\Phi_w\}$ is the same for all $w \geq 0$.

Examples of Pauli-ordered unital qubit queue-channels are depolarising queue-channels [1] and symmetric generalized amplitude damping channels considered in Sec. IV-A.

As discussed before, a queue-channel models decoherence of a qubit due to its interaction with the environment while waiting in a buffer. In this context, it is physically well motivated to work in a Markovian regime, leading to the well known quantum Markov semigroup structure [?] for the channel that models the decoherence. It can be

shown that for a unital qubit queue-channel with a Markov semigroup structure, the Shannon capacities of $B_1(w)$, $B_2(w)$ and $B_3(w)$ do not change with w . Thus, a unital qubit queue-channel with a Markov semigroup structure is indeed Pauli-ordered. This implies that the class of Pauli-ordered unital qubit queue-channels is a physically interesting and broad class of unital qubit queue-channels.

The following lemma is useful in designing an optimal encoding and decoding for Pauli-ordered unital qubit queue channels.

Lemma 4. *For a Pauli-ordered unital qubit queue-channel there exists a Pauli state $\hat{\sigma}$ such that for all $w \geq 0$, $(I + \hat{\sigma})/2 \in \mathcal{R}_{\Phi_w}$. This, in turn, implies that for any $w \geq 0$, $(I + \hat{\sigma})/2 \in \Gamma_{\Phi_w, (I + \hat{\sigma})/2}$.*

Proof of this lemma is presented later. Here, we first derive an optimal product encoding and decoding strategy using this lemma.

Encoding and decoding: We pick a capacity achieving encoder and decoder for the classical binary symmetric queue-channel $\{\text{BSC}(M_{\Phi_{W_i}})\}$. We map the message to a string of 0 and 1 using that encoder. Then, we map 0 to $(I + \hat{\sigma})/2$ and 1 to $(I - \hat{\sigma})/2$ and use the projective measurement $\{(I - \hat{\sigma})/2, (I + \hat{\sigma})/2\}$ on the output states to obtain strings of 0 and 1. Finally, we use the capacity achieving decoder for the classical binary symmetric queue-channel $\{\text{BSC}(M_{\Phi_{W_i}})\}$ to decode the message.

Theorem 5. *The above product encoding and product decoding strategy achieves the capacity upper-bound in Theorem 2 for Pauli-ordered unital qubit queue-channels.*

Proof. Lemma 4 implies that the above product encoding and decoding strategy converts a Pauli-ordered unital qubit queue-channel into a binary symmetric queue-channel with crossover probabilities

$$\text{Tr}(\Phi_{W_i} ((I + \hat{\sigma})/2) (I + \hat{\sigma})/2) = M_{\Phi_{W_i}}.$$

This is because by lemma 4, $(I + \hat{\sigma})/2 \in \mathcal{R}_{\Phi_{W_i}}$ and $(I + \hat{\sigma})/2 \in \Gamma_{\Phi_{W_i}, (I + \hat{\sigma})/2}$. The rest follows from Theorem 4 in [1]. ■

Proof of Lemma 4. First, note that up to local unitaries at the channel input and output, any unital channel can be written as a convex combination of Pauli channels :

$$\Phi(\rho) = (1 - \sum_{i=1}^3 p_i)\rho + \sum_{i=1}^3 p_i \sigma_i \rho \sigma_i,$$

where σ_i are the Pauli matrices (see discussion between Prop. 6.41 and Ex. 6.43 in [8]).

Thus, any Φ_w can be equivalently represented by the three probabilities $\{p_i(w), i = 1, 2, 3\}$, where

$$\Phi_w(\rho) = (1 - \sum_{i=1}^3 p_i(w))\rho + \sum_{i=1}^3 p_i(w) \sigma_i \rho \sigma_i,$$

and $\sum_i p_i(w) \leq 1$.

We prove Lemma 4 using the following lemma, which gives an explicit expression for the optimal encoding and decoding in terms Pauli matrices.

Lemma 6. For a unital channel Φ , given by $\Phi(\rho) = (1 - \sum_{i=1}^3 p_i)\rho + \sum_{i=1}^3 p_i \sigma_i \rho \sigma_i$,

$$(I + \sigma_{i^*})/2 \in \mathcal{R}_\Phi \text{ and } (I + \sigma_{i^*})/2 \in \Gamma_{\Phi, (I + \sigma_{i^*})/2},$$

where

$$i^* = \arg \max_{i \in \{1,2,3\}} |1 - 2 \sum_{j \neq i} p_j|.$$

Lemma 6 is applicable to any Φ_w parametrized by $\{p_i(w)\}$. Thus, if the ordering of $\eta_i(w) = |\sum_{j=1}^3 p_j(w) - p_i(w) - \frac{1}{2}|$ remains unchanged with w , ρ_w^* and τ_w^* remain unchanged with w .

Finally, note that the ordering of $\{\eta_i(w)\}$ are the same as the ordering of the Shannon capacities of $B_i(w)$. To see this, let us first find the crossover probability of $B_i(w)$. Using simple trace calculations, one can show that the crossover probability $b_i(w)$ of the BSC $B_i(w)$ is $p_i + (1 - \sum_{j=1}^3 p_j)$. Thus, its Shannon capacity is $1 - h(b_i(w))$. Note that $1 - h(b) = 0$ at $b = \frac{1}{2}$ and increases monotonically with $|b - \frac{1}{2}|$. Thus, the capacity of $B_i(w)$ is monotonic in $\eta_i(w)$ and hence, ordering of $\eta_i(w)$ remains unchanged with w for a Pauli-ordered unital qubit queue-channel, which completes the proof of this lemma. \blacksquare

Proof of Lemma 6. For any state $\rho = \frac{I}{2} + \sum_{i=1}^3 \frac{\alpha_i}{2} \sigma_i$, where $\sum_{i=1}^3 \alpha_i^2 \leq 1$,

$$\Phi(\rho) = \sum_{i=1}^3 \frac{\alpha_i}{2} (1 - 2 \sum_{j \neq i} p_j) \sigma_i + (1 - \sum_{i=1}^3 p_i) \frac{I}{2}.$$

Thus, $\rho = \frac{1}{2}(I + \vec{\alpha} \cdot \vec{\sigma}) := \frac{1}{2}(I + \sum_{i=1}^3 \alpha_i \sigma_i)$, where $\vec{\alpha} = (\alpha_1, \alpha_2, \alpha_3)$ and $\vec{\alpha} \cdot \vec{\alpha} \leq 1$, the channel output

$$\Phi(\rho) = \frac{1}{2}(I + (\vec{\lambda} * \vec{\alpha}) \cdot \vec{\sigma}),$$

where $\vec{\lambda} = (\lambda_1, \lambda_2, \lambda_3)$, $\lambda_i = 1 - 2 \sum_{j \neq i} p_j$, and $(\vec{\lambda} * \vec{\alpha})_i = \vec{\lambda}_i \vec{\alpha}_i$ denotes entry-wise dot product between $\vec{\lambda}$ and $\vec{\alpha}$. Thus,

$$\begin{aligned} M_\Phi &= \sup_{\{\vec{\alpha}: \vec{\alpha} \cdot \vec{\alpha} \leq 1\}, \text{ pure } \tau} \frac{1}{2} \text{Tr}\{((I + (\vec{\lambda} * \vec{\alpha}) \cdot \vec{\sigma}) \tau)\} \\ &= \sup_{\{\vec{\alpha}: \vec{\alpha} \cdot \vec{\alpha} \leq 1\}, \{\vec{\beta}: \vec{\beta} \cdot \vec{\beta} = 1\}} \frac{1}{4} \text{Tr}\{((I + (\vec{\lambda} * \vec{\alpha}) \cdot \vec{\sigma})(I + \vec{\beta} \cdot \vec{\sigma}))\} \end{aligned}$$

The last step follows from the fact that τ is a pure state.

After doing the matrix products and using some linear algebra involving linearity of trace, and the facts that $\text{Tr}(\sigma_i) = 0$, $\sigma_i^2 = I$, and for $i \neq j$, $\sigma_i \sigma_j = -\sigma_j \sigma_i$, one obtains

$$M_\Phi = \sup_{\{\vec{\alpha}: \vec{\alpha} \cdot \vec{\alpha} \leq 1\}, \{\vec{\beta}: \vec{\beta} \cdot \vec{\beta} = 1\}} \frac{1}{2} (1 + (\vec{\lambda} * \vec{\alpha}) \cdot \vec{\beta}).$$

It follows from the Cauchy-Schwartz inequality that the supremum is obtained when $\vec{\alpha} = \vec{\beta}$ and $|\beta_i| = 1$ for $i = i^* = \text{argmax } |\lambda_i|$. Using the definition of λ_i , it follows that $i^* = \text{argmax } |1 - 2 \sum_{j \neq i} p_j|$. \blacksquare

The notion of Pauli-ordered unital qubit queue-channels is directly connected to the binary i.i.d. classical channels induced by the Pauli matrices. This gives a physical interpretation of the conditions under which the statement in

Theorem 5 holds true. However, a result like Theorem 5, holds for a broader class of unital qubit channels, which can be characterized without using any reference to their Pauli decompositions.

Definition 5. Let $\{\Phi_w\}$ be the class of i.i.d. unital qubit channels corresponding to the unital qubit queue-channels. We call the queue-channel to have a **waiting-invariant norm maximizer** if

$$\bigcap_{w \geq 0} \mathcal{R}_{\Phi_w} \neq \emptyset.$$

This class of queue-channels includes the class of Pauli-ordered queue-channels since it follows directly from Lemma 6 that there exists a Pauli state $\hat{\sigma}$ such that $(I + \hat{\sigma})/2 \in \bigcap_{w \geq 0} \mathcal{R}_{\Phi_w}$.

Encoding and decoding: Let $\bar{\rho}$ be a state in $\bigcap_{w \geq 0} \mathcal{R}_{\Phi_w}$ and $\bar{\tau}_{W_i}$ be a state in $\Gamma_{\Phi_{W_i}, \bar{\rho}}$. We pick a capacity achieving code for the queue-channel BSC ($M_{\Phi_{W_i}}$) and generate classical codes accordingly. Then, we map $\{0, 1\}$ to $\bar{\rho}$ and $I - \bar{\rho}$ and decode the output states using the POVM $\{I - \bar{\tau}_{W_i}, \bar{\tau}_{W_i}\}$. Clearly, the encoder does not depend on individual W_i s, but the decoder may. In that sense also, this strategy is a generalization of the strategy used for Pauli-ordered channels.

Theorem 7. *The above product encoding and product decoding strategy achieves the capacity upper-bound in Theorem 2 for unital qubit queue-channels with a waiting-invariant norm maximizer.*

Proof. It is enough to prove that the above encoding and decoding strategy converts a unital qubit queue-channel with waiting-invariant norm maximizer into a binary symmetric queue-channel $\{\text{BSC}(M_{\Phi_{W_i}})\}$. The rest follows from Theorem 4 in [1].

The crossover probability for state i under this induced channel is given by

$$\text{Tr}(\Phi_{W_i}(\bar{\rho}) \tau_{W_i}) = \text{Tr}(\Phi_{W_i}(\rho) \tau),$$

for $\rho \in \mathcal{R}_{\Phi_{W_i}}$ and $\tau \in \Gamma_{\Phi_{W_i}, \rho}$. Hence, this quantity is equal to $M_{\Phi_{W_i}}$. ■

Clearly, Theorem 7 is more general than Theorem 5 as it is applicable to a broader class of unital qubit queue-channels. However, Lemma 6, which is an intermediate result for Theorem 5, gives a simple closed form encoder and decoder in terms of Pauli matrices. This is of independent interest as it applies to any i.i.d. unital qubit channel as well. Also, we did not come across any practical scenario which may lead to unital queue-channels that are not Pauli-ordered.

IV. QUBIT GENERALIZED AMPLITUDE DAMPING (GAD) QUEUE-CHANNELS

A. I.I.D GAD

The qubit generalized amplitude damping (GAD) channel $\mathcal{A}_{p,n} : \mathcal{L}(\mathcal{H}_a) \mapsto \mathcal{L}(\mathcal{H}_b)$ is a two parameter family of channels where the parameters p and n are between zero and one. The channel has a qubit input and qubit output— $d_a = d_b = 2$ — and its superoperator has the form,

$$\mathcal{A}_{p,n}(\rho) = \sum_{i=0}^3 K_i \rho K_i^\dagger, \tag{17}$$

where

$$K_0 = \sqrt{1-n}|0\rangle\langle 0| + \sqrt{1-p}|1\rangle\langle 1|, \quad K_1 = \sqrt{p(1-n)}|0\rangle\langle 1|, \quad (18)$$

$$K_2 = \sqrt{n}(\sqrt{1-p}|0\rangle\langle 0| + |1\rangle\langle 1|), \quad \text{and} \quad K_3 = \sqrt{pn}|1\rangle\langle 0| \quad (19)$$

are Kraus operators. The GAD (17) channel can also be expressed as

$$\mathcal{A}_{p,n} = (1-n)\mathcal{A}_{p,0} + n\mathcal{A}_{p,1}. \quad (20)$$

The above representation provides the following insightful interpretation. The parameter n represents the mixing of $\mathcal{A}_{p,0}$ with $\mathcal{A}_{p,1}$, where each channel $\mathcal{A}_{p,i}$ ($i = 0$ or 1) is an amplitude damping channel that favours the state $[i]$ (here we use the notation $[\psi]$ for $|\psi\rangle\langle\psi|$) by keeping it fixed and maps the orthogonal state $[1-i]$ to $[i]$ with damping probability p . When $n = 1/2$, $\mathcal{A}_{p,n}$ is unital and we get equal mixing of both $\mathcal{A}_{p,0}$ and $\mathcal{A}_{p,1}$. This equal mixing represents noise where each state $[i]$ ($i = 0, 1$) is mapped to itself with probability $p/2$ and to $[1-i]$ with probability $1-p/2$; in other words, this $n = 1/2$ noise treats both $[0]$ and $[1]$ identically. However, when n is not half, the action of $\mathcal{A}_{p,n}$ on $[0]$ is different from its action on $[1]$. In particular, $[0]$ is mapped to itself with probability $1-pn$ and to $[1]$ with probability pn , and $[1]$ is mapped to itself with probability $1-p(1-n)$ and to $[0]$ with probability $p(1-n)$.

Any qubit density operator can be written in the Bloch parametrization,

$$\rho(\mathbf{r}) = \frac{1}{2}(I + \mathbf{r} \cdot \vec{\sigma}) := \frac{1}{2}(I + x\sigma^x + y\sigma^y + z\sigma^z), \quad (21)$$

where the Bloch vector $\mathbf{r} = (x, y, z)$ has norm $|\mathbf{r}| \leq 1$,

$$\sigma^x = \begin{pmatrix} 0 & 1 \\ 1 & 0 \end{pmatrix}, \quad \sigma^y = \begin{pmatrix} 0 & -i \\ i & 0 \end{pmatrix}, \quad \text{and} \quad \sigma^z = \begin{pmatrix} 1 & 0 \\ 0 & -1 \end{pmatrix} \quad (22)$$

are the Pauli matrices, written in the standard basis $\{|0\rangle, |1\rangle\}$. Using the Bloch parametrization, the entropy

$$S(\rho(\mathbf{r})) = h((1-|\mathbf{r}|)/2), \quad (23)$$

where $h(x) := -[x \log x + (1-x) \log(1-x)]$ is the binary entropy function and $|\mathbf{r}| = \sqrt{\mathbf{r} \cdot \mathbf{r}}$ is the norm of \mathbf{r} . An input density operator $\rho(\mathbf{r})$ is mapped by $\mathcal{A}_{p,n}$ to an output density operator with Bloch vector,

$$\mathbf{r}' = (\sqrt{1-px}, \sqrt{1-py}, (1-p)z + p(1-2n)). \quad (24)$$

The GADC is unital at $n = 1/2$; that is, $\mathcal{A}_{p,1/2}(I) = I$. The GADC is entanglement breaking [9], [26], [46] when

$$2(\sqrt{2}-1) \leq p \leq 1 \quad \text{and} \quad \frac{1}{2}(1-l(p)) \leq n \leq \frac{1}{2}(1+l(p)), \quad (25)$$

where $l(p) = \sqrt{\frac{p^2+4p-4}{p^2}}$. The Holevo capacity of unital qubit channels and entanglement breaking channels is additive; as a result, when $n = 1/2$ or when the values of parameters p and n satisfy (25), the Holevo information of the generalized amplitude damping channel, $\chi^{(1)}(\mathcal{A}_{p,n})$, equals the classical capacity of the channel, $\chi(\mathcal{A}_{p,n})$. For other values of p and n , the classical capacity of the GADC is not known because for these parameter values, the Holevo information of the channel is not known to be additive or non-additive. The actual value of the Holevo information can be computed numerically. Next, we briefly discuss this numerical calculation for completeness.

B. Holevo Information

Let $[\alpha_+]$ and $[\alpha_-]$ be projectors on states with Bloch vector

$$\mathbf{r}_+ = (\sqrt{1-z^2}, 0, z), \quad \text{and} \quad \mathbf{r}_- = (-\sqrt{1-z^2}, 0, z), \quad (26)$$

respectively; here $-1 \leq z \leq 1$. Notice, $[\alpha_+]$ and $[\alpha_-]$ are not orthogonal, except when $z = 0$. It has been shown [27] that the Holevo information,

$$\chi^{(1)}(\mathcal{A}_{p,n}) = \max_{\{-1 \leq z \leq 1\}} S(\mathcal{A}_{p,n}(\sigma)) - [S(\mathcal{A}_{p,n}([\alpha_+])) + S(\mathcal{A}_{p,n}([\alpha_-]))]/2, \quad (27)$$

where $\sigma = ([\alpha_+] + [\alpha_-])/2$. In the above equation, the optimizing z has the value

$$z^* = \frac{u - p(1-2n)}{1-p}, \quad (28)$$

where u comes from solving,

$$(pu - p^2(1-2n) - p(1-p)(1-2n))f'(r^*) = -r^*(1-\gamma)f'(u), \quad (29)$$

with

$$f(x) := (1+x)\log_2(1+x) + (1-x)\log_2(1-x), \quad (30)$$

$$f'(x) = \log_2\left(\frac{1+x}{1-x}\right), \quad \text{and} \quad (31)$$

$$r^* := \sqrt{1-p - \frac{(u-p(1-2n))^2}{1-p} + u^2}. \quad (32)$$

Using the value of z^* in (28) gives,

$$\chi^{(1)}(\mathcal{A}_{p,n}) = \frac{1}{2}(f(r^*) - \log_2(1-u^2) - uf'(u)). \quad (33)$$

Solving (25) for $n \leq 1/2$ gives a range,

$$p^* \leq p \leq 1, \quad (34)$$

where the GAD channel in entanglement breaking. Here the value,

$$p^* = \max\left(2(\sqrt{2}-1), \frac{\sqrt{1+4n(1-n)}-1}{2n(1-n)}\right). \quad (35)$$

As indicated earlier, entanglement breaking channels have additive Holevo capacity. Thus, when p satisfies (34), the GAD channel has additive Holevo capacity. While the Holevo information $\chi^{(1)}(\mathcal{A}_{n,p})$ gives the product state classical channel capacity, it doesn't give an explicit encoding and decoding that achieves this capacity. In what follows, we construct explicit encoding and decodings—in other words, we construct induced classical channels, and compare the capacity of these channels to the product state classical capacity $\chi^{(1)}(\mathcal{A}_{n,p})$. For $n = 1/2$, we find the optimal encoding and decoding which achieves $\chi^{(1)}(\mathcal{A}_{1/2,p})$ for all $0 \leq p \leq 1$.

C. Induced Channels

To obtain an induced channel for $\mathcal{A}_{p,n} : \mathcal{L}(\mathcal{H}_a) \mapsto \mathcal{L}(\mathcal{H}_b)$ one must choose an encoding and decoding. To choose an encoding, $\mathcal{E} : \mathcal{X} \mapsto \mathcal{L}(\mathcal{H}_a)$, one fixes a set of input states $\{\rho(x)\}$. To choose a decoding, $\mathcal{D} : \mathcal{L}(\mathcal{H}_b) \mapsto \mathcal{Y}$, one fixes an output measurement POVM $\{\Lambda(y)\}$. Together this encoding-decoding results in an induced channel with conditional probability $p(y|x) = \text{Tr}(\rho(x)\Lambda(y))$. A priori, there is no clear choice for these input states and output measurement. However, the generalized qubit amplitude damping channel satisfies an equation

$$\mathcal{A}_{p,n}(\sigma_a^z \rho (\sigma_a^z)^\dagger) = \sigma_b^z \mathcal{A}_{p,n}(\rho) (\sigma_b^z)^\dagger, \quad (36)$$

where the subscripts a and b on the Pauli operator σ^z signify the space on which the operator acts. The above equation implies that the generalized amplitude damping channel has a rotational symmetry around the z -axis. Using this rotational symmetry and the fact that $\mathcal{A}_{p,n}$ is a qubit input-output channel one may choose an encoding $\mathcal{E}(x) = \rho(x)$ where $x = 0$ or 1 and $\{\rho(x)\}$ are two orthogonal input states that remain unchanged under the σ_a^z symmetry operations; that is, $\rho(x) = [x]$. To decode, one may apply a protocol for correctly identifying a state chosen uniformly from a set of two known states $\mathcal{A}_{p,n}([0])$ and $\mathcal{A}_{p,n}([1])$ with highest probability. This protocol comes from the theory of quantum state discrimination [49]. It uses a POVM with two elements $\{E, I_b - E\}$, where E is a projector onto the space of positive eigenvalues of $\mathcal{A}_{p,n}([0]) - \mathcal{A}_{p,n}([1])$. An unknown state, either $\mathcal{A}_{p,n}([0])$ or $\mathcal{A}_{p,n}([1])$ with equal probability, is measured using the POVM. If the outcome corresponding to E occurs, the unknown state is guessed to be $\mathcal{A}_{p,n}([0])$; otherwise, the guess is $\mathcal{A}_{p,n}([1])$. In the present case, a simple calculation shows that $E = [0]$.

Encoding $\mathcal{E}(x) = [x]$, ($x = 0, 1$) and decoding based on the POVM $\{[0], [1]\}$, coming from the state discrimination protocol outlined above, results in an induced channel \mathcal{N}_1 . This channel is a BAC that flips $x = 0$ to $y = 1$ with probability pn but flips $x = 1$ to $y = 0$ with probability $p(1 - n)$. Its capacity $C(\mathcal{N}_1)$ has a simple closed form expression (2). For $C(\mathcal{N}_1)$, this expression is unchanged when n is replaced with $1 - n$, thus we may restrict our attention to $0 \leq n \leq 1/2$.

At $n = 1/2$, $\mathcal{A}_{p,n}$ is unital. In Sec. III-B, we defined an induced channel which achieves the Holevo information of any qubit unital channel. On the basis of that induced channel, we may construct an induced channel for values of n different from $1/2$. In this construction the encoding map $\mathcal{E}(0) = \rho^*$, and $\mathcal{E}(1) = I - \rho^*$ (ρ^* defined below eq. (14)); the decoding map \mathcal{D} measures the output of $\mathcal{A}_{p,n}$ using the POVM $\{\tau^*, I - \tau^*\}$ (τ^* defined in eq. (15)) to return 0 when the measurement outcome corresponds to POVM element τ^* , otherwise return 1. This encoding-decoding results in the induced channel \mathcal{N}_2 which is a BAC. This BAC flips input 0 to output 1 with probability $(1 - |\mathbf{r}'|)/2$, $|\mathbf{r}'|^2 = 4n(1-n)(1-p) + (1-2n)^2$ and flips input 1 to output 0 with probability $\frac{1}{2}(1 + \frac{p(1-(1-2n)^2)-1}{|\mathbf{r}'|})$. The channel's capacity, $C(\mathcal{N}_2)$ (computed using expression (2)), remains invariant when n is replaced with $1 - n$. This invariance permits us to restrict ourselves to the parameter range $0 \leq n \leq 1/2$.

Next, we consider a third induced channel. This channel is based on the computation of the Holevo information of $\mathcal{A}_{p,n}$ in Sec. IV-B. Here, encoding is performed using possibly non-orthogonal states and decoding is performed using a measurement designed to distinguish these encoded states at the channel output with maximum probability. The encoding maps $x = 0$ and $x = 1$ to $[\alpha_+]$ and $[\alpha_-]$ (defined via eq. (26)), respectively. The decoding is

performed using a POVM $\{\Lambda(y)\}$ where $\Lambda(y)$ at $y = 0$ is the projector onto the space of positive eigenvalues of $\mathcal{A}_{p,n}([\alpha_+]) - \mathcal{A}_{p,n}([\alpha_-])$. This projector is simply $[x_+]$, where $|x_+\rangle := (|0\rangle + |1\rangle)/\sqrt{2}$. This encoding-decoding scheme results in a one-parameter family of induced channels $\mathcal{N}_3(z)$. This channel is a BSC with flip probability $q(z) = (1 - a(z)\sqrt{1-p})/2$, where $a(z) = \sqrt{1-z^2}$. Interestingly, this family of induced channels, coming from the two parameter GAD channel $\mathcal{A}_{p,n}$, does not depend on the parameter n . The Shannon capacity of $\mathcal{N}_3(z)$ is simply

$$C(\mathcal{N}_3(z)) = 1 - h(q(z)). \quad (37)$$

For a fixed p , one can easily show that $C(\mathcal{N}_3(z))$ is maximum when $z = 0$; thus, $\mathcal{N}_3 = \mathcal{N}_3(0)$ has the largest Shannon capacity among the one-parameter family of induced channels $\mathcal{N}_3(z)$. This induced channel \mathcal{N}_3 is simply a BSC with flip probability $q = (1 - \sqrt{1-p})/2$.

We compare the capacities of the three induced channels \mathcal{N}_1 , \mathcal{N}_2 , and \mathcal{N}_3 . As mentioned earlier, we can restrict ourselves to $0 \leq n \leq 1/2$. A straightforward calculation shows that at $n = 0$, \mathcal{N}_1 and \mathcal{N}_2 are equivalent up to permutation of the inputs and output and thus $C(\mathcal{N}_1) = C(\mathcal{N}_2)$. In general, $0 \leq n \leq 1/2$, here simple numerics can be used to show that

$$C(\mathcal{N}_1) \leq C(\mathcal{N}_2) \leq C(\mathcal{N}_3). \quad (38)$$

All inequalities above are numerically found to be strict when $0 < n < 1/2$ and $0 < p < 1$. At $n = 1/2$, \mathcal{N}_2 and \mathcal{N}_3 become identical, they are both BSC with flip probability $q = (1 - \sqrt{1-p})/2$. This flip probability can be easily shown to equal $\mathcal{N}_{\mathcal{A}_{p,1/2}}$ (defined in eq. (14)). Using this equality, or the fact that $\mathcal{N}_2 = \mathcal{N}_3$ is the induced channel which achieves the Holevo information when $\mathcal{A}_{p,n}$ is unital at $n = 1/2$, we conclude $C(\mathcal{N}_3) = \chi^{(1)}(\mathcal{A}_{p,1/2})$.

For values of $n < 1/2$ we compare the capacity of the \mathcal{N}_3 , the induced channel with the largest capacity among \mathcal{N}_1 , \mathcal{N}_2 , and \mathcal{N}_3 with $\chi^{(1)}(\mathcal{A}_{p,n})$. We numerically find that for values of $n < 1/2$ and $0 < p < 1$, $C(\mathcal{N}_3) < \chi^{(1)}(\mathcal{A}_{p,n})$ (see Fig. 2).

In what follows, we focus on the $n = 1/2$ GADC $\mathcal{A}_{p,1/2}$. As discussed below (20), this channel describes noise in which both computational basis states $|0\rangle$ and $|1\rangle$ are treated on equal footing. When information about which of these computational basis states decays faster than the other, the GADC with $n \neq 1/2$ is an apt noise model. However when such information is unavailable, or when it is known that both computational basis states decay but the maximally mixed state doesn't, one uses the $n = 1/2$ GADC. One simple example of such noise is the qubit thermal channel (analogous to the bosonic thermal channel [23], [24], [26]) in which the channel environment is represented by the maximally mixed state. Another simple example is the effect of dissipation to an environment at a finite temperature [7].

D. Capacity of the symmetric GAD queue-channel

For a symmetric GADC, the parameter p captures the level of damping experienced by a qubit while interacting with an environment. In the absence of buffer decoherence, p depends on the flight time T_f through the channel and the physical parameters of the channel. Similarly, the level of damping experienced in the buffer depends on the waiting time in the buffer W and the physical parameters of the buffer. Hence, the effective GADC parameter

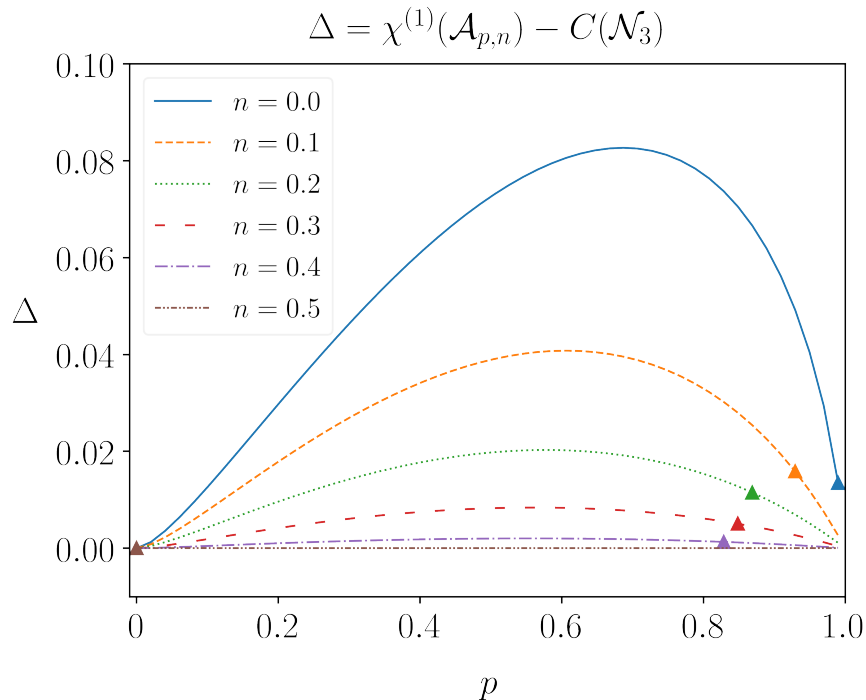


Fig. 2: The difference $\Delta = \chi^{(1)}(\mathcal{A}_{p,n}) - C(\mathcal{N}_3)$ as a function of p for various values of the parameter n . For each n , the colored triangle indicates the value of p^* above which $\chi^{(1)}(\mathcal{A}_{p,n})$ is additive.

experienced by a qubit is a function $g(T_f, W)$ of its waiting time and its flight time, where the form of $g(\cdot)$ depends on the physical parameters of the channel and the buffer. As the flight time is almost deterministic, for simplicity of notations we denote this function by $p_{\text{eff}}(W)$.

The capacity of a symmetric GAD queue-channel can be expressed as follows.

Theorem 8. *The capacity of a symmetric GAD queue-channel is*

$$\lambda \mathbf{E}_\pi \left[1 - h \left(\frac{1 - \sqrt{1 - p_{\text{eff}}(W)}}{2} \right) \right].$$

Proof. As shown in Sec. IV-C, the optimal encoding and the optimal POVM for symmetric GAD channels do not change with the channel parameter p . Thus, the symmetric GAD queue-channel allows a time-invariant encoding. Hence, Theorem 7 for unital qubit queue-channel with time invariant encoding is applicable to symmetric GAD queue-channels with parameter $p_{\text{eff}}(W)$.

The rest follows by noting that the induced classical channel of a symmetric GAD channel with parameter p is a binary symmetric channel with flip probability $(1 - \sqrt{1 - p})/2$. ■

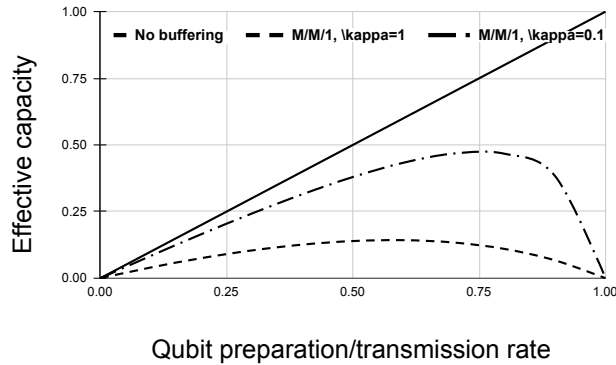


Fig. 3: Capacity (effective) vs qubit preparation rate (λ) for different buffer decoherence.

E. Useful design insights

As the motivation for this work is the practical issues faced by current quantum networks, we discuss few important practical insights obtained from the analytical results for symmetric GAD queue-channels.

In Fig. 3, the capacity per unit time (in contrast to per channel use) of an idealized i.i.d symmetric GADC with $p = 0$ is plotted (no buffering) against the qubit preparation rate. This has the misleading implication that the higher the qubit preparation rate, the higher is the capacity. However, it is well known that in any practical system, especially at a high qubit preparation rate, there will be significant buffering at the transmitter, which will result in additional decoherence of qubits, of significant magnitude, thus, resulting in the loss of capacity. This is a fundamental concept in communication network design.

To illustrate this, we use a simple queue-channel model involving the well known M/M/1 queue [50] that can analytically capture the loss in capacity at a high qubit preparation rate due to buffering. In Fig. 3, two such plots are shown for symmetric GADC with M/M/1 buffering and exponential decoherence

$$p_{\text{eff}}(W) = 1 - \exp(-\kappa W), \quad (39)$$

with mean decoherence time κ^{-1} . We obtain these plots using the capacity expression in Theorem 2.

Clearly, in Fig. 3, the optimal λ is not close to $\mu (= 1)$. Moreover, for λ close μ , the capacity is almost zero. This is because very high λ leads to large waiting times for qubits and thus results in significant decoherence. Furthermore, the optimal λ depends on κ and hence, on the physical parameters of the buffer. The idealized i.i.d. setting fails to capture this crucial dependence.

In general, obtaining a closed form expression for the best λ is not possible. However, for any buffering discipline, the best λ can be obtained by solving

$$\arg \max_{\lambda \in (0, \mu)} \lambda \mathbf{E}_{\pi} \left[1 - h \left(\frac{1 - \sqrt{1 - p_{\text{eff}}(W)}}{2} \right) \right].$$

Though it may appear that the capacity expression increases with λ , it is not so since $\pi(\cdot)$ depends on λ .

F. Optimal queuing distributions

The effective capacity in the presence of buffer decoherence is a function of the stationary distribution of waiting times. Thus, in turn, it is heavily influenced by the time between preparation of two qubits and the time to process (transmit and receive) a qubit. A quantitative understanding of this dependence is useful for designing quantum communication systems.

In this section, we take a short stride in that direction by characterizing the optimal distributions in two queuing settings of general interest when the channel and buffer decoherence follows the exponential model in Eq. 39. The exponential decoherence model is physically the most well motivated model for capturing decoherence in terms of the interaction time with the environment.

First, we obtain a simpler expression of the capacity result in Theorem 8 for the exponential decoherence model.

Corollary 9. *The effective capacity in the presence of buffer decoherence is given by*

$$\frac{\lambda}{\ln 2} \sum_{k=1}^{\infty} \frac{1}{2k(2k-1)} \mathbb{E}_{W \sim \pi} [\exp(-\kappa k W)],$$

when $p_{\text{eff}}(W) = 1 - \exp(-\kappa W)$ for some $\kappa > 0$.

Proof. For the exponential decoherence model, the capacity expression in Theorem 8 becomes

$$\lambda \mathbf{E}_{\pi} \left[1 - h \left(\frac{1 - \exp(-\frac{1}{2}\kappa W)}{2} \right) \right].$$

The rest follows using the series expansion of $\log(1+x)$ for $|x| < 1$ and algebraic manipulations. ■

Note that the expression in Cor. 9 is valid for any stable queue, irrespective of the queuing discipline and distributions.

In the queuing literature, M/G/1 and G/M/1 are two popular classes of queuing models. In our setting, M/G/1 is equivalent to exponentially distributed (memoryless) preparation times and generally distributed processing or service times of qubits. G/M/1 is equivalent to generally distributed preparation times and exponentially distributed processing or service times. As a first step towards optimizing queuing distributions, one may ask: what are the best distribution for processing times and preparation times in M/G/1 and G/M/1 queues, respectively? The following theorems answer this question.

Theorem 10. *Among all quantum communication systems with M/G/1 buffering, symmetric GAD channel, and exponential decoherence, the system with deterministic processing or service time has the maximum effective capacity for any λ and $\mu (> \lambda)$.*

Proof. Suppose there exists a service distribution for which $\mathbb{E}_{W \sim \pi} [\exp(-sW)]$ is more than any other service distribution with the same mean for any $s > 0$. Then, from the capacity expression in Corollary 9, it is clear that under that particular distribution, each term in the series will be greater than the corresponding term for any other distribution. Hence, that distribution will achieve the maximum capacity among the class of all service distributions with the same mean.

Thus, to complete this proof, we need only to show that for exponentially distributed preparation times, the deterministic service time maximizes $\mathbb{E}_{W \sim \pi} [\exp(-sW)]$ for any $s > 0$. This follows directly from the proof of Theorem 4 in [1]. ■

Theorem 11. *Among all quantum communication systems with G/M/1 buffering, symmetric GAD channel, and exponential decoherence, the system with deterministic preparation/arrival time has the maximum effective capacity for any λ and $\mu (> \lambda)$.*

Proof. Using the argument in the proof of Theorem 10, it is sufficient to show that for exponentially distributed service times, the deterministic preparation/arrival time maximizes $\mathbb{E}_{W \sim \pi} [\exp(-sW)]$ for any $s > 0$.

The following two lemmas complete the proof of this theorem.

Lemma 12. *Among all arrival/preparation distributions with mean $\lambda^{-1} (> \mu^{-1})$, $\mathbb{E}_{W \sim \pi} [\exp(-sW)]$ for any $s > 0$ is maximized by that arrival/preparation distribution for which the solution to the G/M/1 fixed point equation*

$$\sigma = \mathbb{E}_A [\exp(-(\mu - \mu \sigma) A)]$$

is the smallest.

Lemma 13. *Among all arrival/preparation distributions with mean $\lambda^{-1} (> \mu^{-1})$, the solution to the G/M/1 fixed point equation*

$$\sigma = \mathbb{E}_A [\exp(-(\mu - \mu \sigma) A)]$$

is the smallest for the deterministic arrival/preparation time λ^{-1} .

■

Proof of Lemma 12. The waiting time in a G/M/1 queue is exponentially distributed with mean $\frac{1}{\mu(1-\sigma)}$, where σ is the solution to the fixed point equation

$$\sigma = \mathbb{E}_A [\exp(-(\mu - \mu \sigma) A)].$$

For exponentially distributed W , $\mathbb{E} [\exp(-sW)]$ decreases with $\mathbb{E}[W]$. Hence, for a given μ , $\mathbb{E} [\exp(-sW)]$ increases as σ decreases, which, in turn, implies Lemma 12. ■

Proof of Lemma 13 is similar to the proof of Proposition 2 in [34].

V. CONCLUSION AND OUTLOOK

Understanding the classical capacity of a quantum channel and the means by which it can be achieved are fundamental issues in quantum information theory. We derived an explicit capacity-achieving non-entangled projective measurement strategy for i.i.d unital qubit channel. This implies that the classical capacity of a unital qubit channel can be achieved without entanglement using essentially classical resources.

Building on this insight, we showed that non-entangled projective measurements achieve the classical capacity of a broad class of unital qubit queue-channels that includes the well known unital qubit queue-channels like Pauli

channels and symmetric generalized amplitude damping channels. In the special case of the symmetric generalized amplitude damping channel, we show that our result on unital qubit channel allows one to pick the capacity achieving product encoding-decoding strategy (induced channel) out of a few natural yet sub-optimal choices.

By taking the symmetric generalized amplitude damping channel as an example, we demonstrate that ignoring the effect of decoherence in the buffer can lead to an erroneous design choice. On the other hand, a queue-channel based analysis, which offers a succinct model for decoherence in the buffer, gives a procedure for finding the optimal operating point.

For operating a practical quantum communication system close to its capacity, efficient error correcting codes are essential. Our results from Sec. III imply that any capacity achieving classical error correcting code for binary symmetric channels, e.g., polar code, achieves the classical capacity of i.i.d. unital qubit channels. They also imply that a capacity achieving code for classical binary symmetric queue-channels achieves the classical capacity of unital qubit queue-channels when used in conjunction with the proposed product (classical to quantum) encoder and decoder. However, though the existence of a capacity achieving code for classical binary symmetric queue-channels is known [1], [34], the question of explicitly and efficiently finding such a code remains open.

Another important question follows from our work: can we construct induced classical channels for non-unital quantum channels with additive Holevo information? Obtaining such capacity achieving constructions remains an interesting open problem. To solve such a problem, one may follow the method in this work. To use this method, one starts with a quantum channel with additive Holevo information and then constructs an explicit induced channel which achieves this Holevo information. As demonstrated in Sec. IV-A using the GADC, induced channels of this type can be non-trivial to construct. For instance, in the case of non-unital GADC channels with additive Holevo information, finding such induced channels remains an open problem. In addition, finding the full parameter region where the GADC has additive Holevo information also remains open.

Insights obtained from pursuing such open problems have the potential to not only enrich the i.i.d setting with point-to-point quantum channels but also provide a path to study non-i.i.d queue channel settings that arise in quantum networks. Another challenging avenue for future work is to characterise the queue channel capacity when the underlying noise model is not additive, as could be the case for certain parameter ranges of the GADC. This may require a fundamentally new approach to study quantum communication networks.

ACKNOWLEDGMENTS

The authors thank Mark M. Wilde for useful comments on a previous draft of this work. VS gratefully acknowledges support from NSF CAREER Award CCF 1652560 and NSF grant PHY 1915407. The work of AC was supported in part by the Department of Science and Technology, Government of India under Grant SERB/SRG/2019/001809 and Grant INSPIRE/04/2016/001171. PM and KJ acknowledge the Metro Area Quantum Access Network (MAQAN) project, supported by the Ministry of Electronics and Information Technology, India vide sanction number 13(33)/2020-CC&BT.

REFERENCES

- [1] P. Mandayam, K. Jagannathan, and A. Chatterjee. The classical capacity of additive quantum queue-channels. *IEEE Journal on Selected Areas in Information Theory*, 1(2):432–444, Aug 2020. doi:10.1109/JSAIT.2020.3015055.
- [2] Stefano Pirandola and Samuel L. Braunstein. Physics: Unite to build a quantum internet. *Nature*, 532:169–171, Apr 2016. doi:10.1038/532169a.
- [3] Wojciech Kozłowski, Axel Dahlberg, and Stephanie Wehner. Designing a quantum network protocol. In *Proceedings of the 16th International Conference on Emerging Networking EXperiments and Technologies*, CoNEXT '20, page 1–16, New York, NY, USA, 2020. Association for Computing Machinery. doi:10.1145/3386367.3431293.
- [4] Kae Nemoto, Michael Trupke, Simon J Devitt, Burkhard Scharfenberger, Kathrin Buczak, Jörg Schmiedmayer, and William J Munro. Photonic quantum networks formed from nv^- centers. *Scientific reports*, 6(1):1–12, 2016.
- [5] F Rozpędek, K Goodenough, J Ribeiro, N Kalb, V Caprara Vivoli, A Reiserer, R Hanson, S Wehner, and D Elkouss. Parameter regimes for a single sequential quantum repeater. *Quantum Science and Technology*, 3(3):034002, apr 2018. doi:10.1088/2058-9565/aab31b.
- [6] E. Shchukin, F. Schmidt, and P. van Loock. Waiting time in quantum repeaters with probabilistic entanglement swapping. *Phys. Rev. A*, 100:032322, Sep 2019. doi:10.1103/PhysRevA.100.032322.
- [7] Michael A. Nielsen and Isaac L. Chuang. *Quantum Computation and Quantum Information: 10th Anniversary Edition*. Cambridge University Press, New York, NY, USA, 10th edition, 2011.
- [8] Alexander S. Holevo. *Quantum Systems, Channels, Information: A Mathematical Introduction*. De Gruyter, 2012. doi:10.1515/9783110273403.
- [9] Christopher King. Additivity for unital qubit channels. *Journal of Mathematical Physics*, 43(10):4641–4653, 2002. doi:10.1063/1.1500791.
- [10] Nilanjana Datta and Mary Beth Ruskai. Maximal output purity and capacity for asymmetric unital qudit channels. *Journal of Physics A: Mathematical and General*, 38(45):9785–9802, Oct 2005. doi:10.1088/0305-4470/38/45/005.
- [11] Motohisa Fukuda and Gilad Gour. Additive bounds of minimum output entropies for unital channels and an exact qubit formula. *IEEE Transactions on Information Theory*, 63(3):1818–1828, 2017. doi:10.1109/TIT.2016.2641455.
- [12] Nicolas Gillard, Étienne Belin, and François Chapeau-Blondeau. Stochastic resonance with unital quantum noise. *Fluctuation and Noise Letters*, 18(03):1950015, 2019. doi:10.1142/S0219477519500159.
- [13] Christopher King. Hypercontractivity for semigroups of unital qubit channels. *Communications in Mathematical Physics*, 328(1):285–301, May 2014. doi:10.1007/s00220-014-1982-4.
- [14] Christian B. Mendl and Michael M. Wolf. Unital quantum channels – convex structure and revivals of birkhoff’s theorem. *Communications in Mathematical Physics*, 289(3):1057–1086, Aug 2009. doi:10.1007/s00220-009-0824-2.
- [15] Charles H. Bennett, Christopher A. Fuchs, and John A. Smolin. *Entanglement-Enhanced Classical Communication on a Noisy Quantum Channel*, pages 79–88. Springer US, Boston, MA, 1997. doi:10.1007/978-1-4615-5923-8_9.
- [16] Christopher A. Fuchs. Nonorthogonal quantum states maximize classical information capacity. *Phys. Rev. Lett.*, 79:1162–1165, Aug 1997. doi:10.1103/PhysRevLett.79.1162.
- [17] Christopher King, Michael Nathanson, and Mary Beth Ruskai. Qubit channels can require more than two inputs to achieve capacity. *Phys. Rev. Lett.*, 88:057901, Jan 2002. doi:10.1103/PhysRevLett.88.057901.
- [18] H. Yuen and J. Shapiro. Optical communication with two-photon coherent states—part i: Quantum-state propagation and quantum-noise. *IEEE Transactions on Information Theory*, 24(6):657–668, 1978. doi:10.1109/TIT.1978.1055958.
- [19] Jeffrey H. Shapiro. The quantum theory of optical communications. *IEEE Journal of Selected Topics in Quantum Electronics*, 15(6):1547–1569, 2009. doi:10.1109/JSTQE.2009.2024959.
- [20] Wen-Jie Zou, Yu-Huai Li, Shu-Chao Wang, Yuan Cao, Ji-Gang Ren, Juan Yin, Cheng-Zhi Peng, Xiang-Bin Wang, and Jian-Wei Pan. Protecting entanglement from finite-temperature thermal noise via weak measurement and quantum measurement reversal. *Phys. Rev. A*, 95:042342, Apr 2017. doi:10.1103/PhysRevA.95.042342.
- [21] F Rozpędek, K Goodenough, J Ribeiro, N Kalb, V Caprara Vivoli, A Reiserer, R Hanson, S Wehner, and D Elkouss. Parameter regimes for a single sequential quantum repeater. *Quantum Science and Technology*, 3(3):034002, Apr 2018. doi:10.1088/2058-9565/aab31b.
- [22] Isaac L. Chuang and M. A. Nielsen. Prescription for experimental determination of the dynamics of a quantum black box. *Journal of Modern Optics*, 44(11-12):2455–2467, 1997. doi:10.1080/09500349708231894.
- [23] C. J. Myatt, B. E. King, Q. A. Turchette, C. A. Sackett, D. Kielpinski, W. M. Itano, C. Monroe, and D. J. Wineland. Decoherence of quantum superpositions through coupling to engineered reservoirs. *Nature*, 403(6767):269–273, Jan 2000. doi:10.1038/35002001.

- [24] Q. A. Turchette, C. J. Myatt, B. E. King, C. A. Sackett, D. Kielpinski, W. M. Itano, C. Monroe, and D. J. Wineland. Decoherence and decay of motional quantum states of a trapped atom coupled to engineered reservoirs. *Phys. Rev. A*, 62:053807, Oct 2000. doi:10.1103/PhysRevA.62.053807.
- [25] Luca Chirolli and Guido Burkard. Decoherence in solid-state qubits. *Advances in Physics*, 57(3):225–285, 2008. doi:10.1080/00018730802218067.
- [26] Sumeet Khatri, Kunal Sharma, and Mark M. Wilde. Information-theoretic aspects of the generalized amplitude-damping channel. *Phys. Rev. A*, 102:012401, Jul 2020. doi:10.1103/PhysRevA.102.012401.
- [27] Hou Li-Zhen and Fang Mao-Fa. The holevo capacity of a generalized amplitude-damping channel. *Chinese Physics*, 16(7):1843–1847, jul 2007. doi:10.1088/1009-1963/16/7/006.
- [28] John Cortese. Relative entropy and single qubit holevo-schumacher-westmoreland channel capacity. *arXiv e-prints*, pages quant-ph/0207128, July 2002, quant-ph/0207128.
- [29] Dominic W. Berry. Qubit channels that achieve capacity with two states. *Phys. Rev. A*, 71:032334, Mar 2005. doi:10.1103/PhysRevA.71.032334.
- [30] Mark M. Wilde. From classical to quantum shannon theory. *arXiv e-prints*, July 2019, 1106.1445v8.
- [31] Filippo Caruso, Vittorio Giovannetti, Cosmo Lupo, and Stefano Mancini. Quantum channels and memory effects. *Reviews of Modern Physics*, 86(4):1203, 2014.
- [32] Masahito Hayashi and Hiroshi Nagaoka. General formulas for capacity of classical-quantum channels. *IEEE Transactions on Information Theory*, 49(7):1753–1768, 2003.
- [33] Krishna Jagannathan, Avhishek Chatterjee, and Prabha Mandayam. Qubits through queues: The capacity of channels with waiting time dependent errors. In *2019 National Conference on Communications (NCC)*, pages 1–6. IEEE, 2019.
- [34] Avhishek Chatterjee, Daewon Seo, and Lav R Varshney. Capacity of systems with queue-length dependent service quality. *IEEE Transactions on Information Theory*, 63(6):3950–3963, 2017.
- [35] Wenhan Dai, Tianyi Peng, and Moe Z Win. Quantum queuing delay. *IEEE Journal on Selected Areas in Communications*, 38(3):605–618, 2020.
- [36] Mihir Pant, Hari Krovi, Don Towsley, Leandros Tassioulas, Liang Jiang, Prithwish Basu, Dirk Englund, and Saikat Guha. Routing entanglement in the quantum internet. *npj Quantum Information*, 5(1):1–9, 2019.
- [37] Gayane Vardoyan, Saikat Guha, Philippe Nain, and Don Towsley. On the stochastic analysis of a quantum entanglement distribution switch. *IEEE Transactions on Quantum Engineering*, 2:1–16, 2021. doi:10.1109/TQE.2021.3058058.
- [38] A. S. Holevo. The capacity of the quantum channel with general signal states. *IEEE Transactions on Information Theory*, 44(1):269–273, Jan 1998. doi:10.1109/18.651037.
- [39] Benjamin Schumacher and Michael D. Westmoreland. Sending classical information via noisy quantum channels. *Phys. Rev. A*, 56:131–138, Jul 1997. doi:10.1103/PhysRevA.56.131.
- [40] Masahide Sasaki, Stephen M. Barnett, Richard Jozsa, Masao Osaki, and Osamu Hirota. Accessible information and optimal strategies for real symmetrical quantum sources. *Phys. Rev. A*, 59:3325–3335, May 1999. doi:10.1103/PhysRevA.59.3325.
- [41] P. W. Shor. The adaptive classical capacity of a quantum channel, or information capacities of three symmetric pure states in three dimensions. *IBM Journal of Research and Development*, 48(1):115–137, 2004. doi:10.1147/rd.481.0115.
- [42] Christopher King and Mary Beth Ruskai. Capacity of quantum channels using product measurements. *Journal of Mathematical Physics*, 42(1):87–98, 2001. doi:10.1063/1.1327598.
- [43] M. B. Hastings. Superadditivity of communication capacity using entangled inputs. *Nat Phys*, 5(4):255–257, Apr 2009. doi:10.1038/nphys1224.
- [44] C. King. The capacity of the quantum depolarizing channel. *IEEE Transactions on Information Theory*, 49(1):221–229, Jan 2003. doi:10.1109/TIT.2002.806153.
- [45] Christopher King, Keiji Matsumoto, Michael Nathanson, and Mary Beth Ruskai. Properties of conjugate channels with applications to additivity and multiplicativity. *Markov Process and Related Fields*, 13:391–423, 2007. <http://math-mpfr.org/journal/articles/id1123/>.
- [46] Peter W. Shor. Additivity of the classical capacity of entanglement-breaking quantum channels. *Journal of Mathematical Physics*, 43(9):4334–4340, 2002. doi:10.1063/1.1498000.
- [47] T. S. Han. *Information-spectrum Methods in Information Theory*. Springer-Verlag Berlin Heidelberg, 2003.
- [48] Sergio Verdú and T. S. Han. A general formula for channel capacity. *IEEE Transactions on Information Theory*, 40(4):1147–1157, 1994.

- [49] Carl W. Helstrom. Quantum detection and estimation theory. *Journal of Statistical Physics*, 1(2):231–252, Jun 1969. doi:10.1007/BF01007479.
- [50] Leonard Kleinrock. *Queuing Systems, Volume I: Theory*. John Wiley & Sons, Inc., 1975.